Mathematical modeling reveals the mechanisms of feedforward regulation in cell fate decisions in budding yeast

Wenlong Li[1], Ming Yi[2,3] *and Xiufen Zou[1*]
1. School of Mathematics and Statistics, Wuhan University, Wuhan 430072, P. R. China
2. Wuhan Institute of Physics and Mathematics, Chinese Academy of Sciences, Wuhan 430071, P.R. China.
3. Department of Physics, College of Science, Huazhong Agricultural University, Wuhan 430070, P. R. China

Detailed network description

First, the cell cycle subsystem of budding yeast in the G1 phase is illustrated in the left region of Figure S1. Cell cycle commitment is initialed by the G1 cyclin Cln3, which is activated when combined with cyclin-dependent-kinase (CDK or Cdc28). The complex Cln3-Cdc28 activates the transcription factors SBF (Swi4/Swi6) and MBF (Mbp1/Swi6) by phosphorylating Whi5, which is bound to them [1, 2]. The phosphorylated Whi5 (Whi5P) is removed from the nucleus, and the activated transcription factors SBF (SBFA) and MBF (MBFP) start the transcription of Cln1/2 and Clb5/6 [3]. Cln1/2 is activated by combining with CDK (Cdc28) (Cln1/2-Cdc28), and Clb5/6 is inhibited by combining with the Sic1 protein [4, 5]. On the one hand, Cln1/2-Cdc28 activates SBF and MBF together with Cln3-Cdc28, which forms a positive feedback loop. On the other hand, Cln1/2 degrades Far1. Thus, Cln1/2 will accumulate rapidly, and Whi5P will be exported form the nucleus rapidly [6, 7]. Recent studies have shown that when approximately half of Whi5 (52%±3%) has been exported, the cell can pass through the Start point, also known as the commitment point [6]. Due to the inhibitor Sic1, Clb5/6 is inactive throughout the G1 phase until Sic1 is degraded at the G1/S transition point [8]. Sic1 has nine consensus CDK phosphorylation sites, and the phosphorylation of multiple sites is required for the SCF ubiquitin ligase F-box protein Cdc4 to efficiently recognize Sic1, thereby targeting it for degradation by the 26S proteasome [5, 8-10]. When more than six sites are phosphorylated by accumulated Cln1/2-Cdc28, Sic1 is degraded from Clb5/6, and Clb5/6 is activated by combining with CDK (Cdc28). Clb5/6-Cdc28 phosphorylates Sic1 together with Cln1/2-Cdc28, forming another positive feedback loop [11, 12]. Meanwhile, Clb5/6-Cdc28 activates SBF and MBF. The cell will pass through the G1/S point and enter S phase when Sic1 is degraded completely [11]. For simplicity, the three-node motif consisting of Cln1/2, Sic1 and Clb5/6 is denoted as the Cln1/2-Sic1-Clb5/6 motif.

Second, we demonstrate the pheromone-induced MAPK pathway subsystems in the right region of Figure S1. There exist a mating pathway in budding yeast cell which is a mitogen-activated protein kinase (MAPK) cascade and it arrests the cell cycle prior to DNA replication primarily by inhibiting G1 cyclins in complex with the cyclin-dependent kinase [6, 13]. As we all know, there exists two types of budding yeast, MATa and MATα. Cells of MATα secrete α-factor and MATa secrete a-factor, respectively. α-factor and a-factor are pheromone. When they are received by cells of opposite type, the mating pathway is activated. Take a cell of MATa as example, pheromone α-factor (secreted by another cell of MATα) binds a receptor Ste2 located in plasma membrane, then activates a heterotrimeric G protein by dissociating G_{α} from $G_{\alpha\beta\gamma}$. $G_{\beta\gamma}$ and Ste20 bind to Ste5 which is a scaffold protein binding Ste11, Ste7, Fus3, resulting in the beginning of the MAPK cascade [14-16]. In MAPK cascade, Ste11 (MAPKKK) phosphorylates Ste7 (MAPKK), Then Ste7 phosphorylates Fus3 (MAPK) [6, 17-19].

Finally, we focus our attentions on the crosstalk between the two subsystems above. The cell cycle subsystem and MAPK pathway subsystem are interacted with each other by Ste5 and a

motif consisting of Far1, Fus3 and Ste12. When downstream MAPK Fus3 is phosphorylated (Fus3PP), it begins to activate Far1 and Ste12 which is the transcription factor of Far1 [20, 21]. Then, Ste12 transcribes Far1, which is a very slow process relative to Far1 being directly activated by Fus3PP and they are not on the same scale [22]. Those three components form a coherence feedforward regulation, for simplicity, it is denoted with Fus3-Far1- Ste12 motif). The activated Far1 (Far1PP) inhibits Cln1/2 by promoting the degradation of it [13], cell arrest prior to entering start point by this way. Meanwhile, Cln1/2 try to inhibit the mating pathway by promoting the degradation of Far1 and detaching the scaffold protein Ste5 from membrane by phosphorylating it, which reversibly localizes to the membrane at the shmoo tip to mediate pheromone signaling [19, 22-25]. The detaching of Ste5 from membrane leads to the disruption of signaling [18]. Those biochemical reactions and interactions are very important for the flexibility of cell fate decision and stability of cellular state [6, 7]. Hence, we will put more emphasis on them in our mathematical model.

Time courses of biomarker-like proteins and Start point in cycling cells

The addition of 240 nM pheromone to WT cells at various times results in different cell fates, as shown in Figure S2. When the pheromone is added before 3 min (Figure S2 B and C), the proteins Ste5mem and Fus3PP are produced at high levels, indicating mating arrest. Most of the Ste5 is recruited to the cell membrane. By contrast, when the pheromone is added after 3 min (Figure S2 D) or when no pheromone is added (Figure S 2 A), the proteins Cln1/2 and SBF are produced at high levels, and the level of Whi5 decreases; these changes imply cell cycle commitment. No Ste5 or only a small fraction of Ste5 is moved to the cell membrane; thus, the MAPK cascade is shut off. Apparently, during the competition between the two groups of proteins, once one cell fate dominates, the proteins representing the other cell fate are suppressed completely[26]. The results from our theoretical model reproduce quantitatively the experimental observations [6].

In our simulation, cell fates are inferred through original method that determines the Start point. This method is reasonable because the kinetics of the pheromone pathway, media switching and Whi5 kinetics are fast (approximately 5 min in total) compared with the G1 duration (30 ~40 min). Our calculation indicates that there is a sharp transition point at 3 min (i.e., the critical addition time is 3 min.), and the Whi5-threshold is 0.48, as shown in Figure S3. This result is consistent with the experimental observation that the Start point occurs when approximately half of Whi5-GFP (52±3%) has been exported [6, 22].

Time courses of biomarker-like proteins in pheromone-arrested cells

Similarly, pheromone-arrested cells are disturbed by adding 240 nM pheromone at different time. To record the state of pheromone-arrested cells, Cln1/2 and Whi5 are chosen to represent the Reentry and mating arrest, while Clb5/6 and Sic1are selected to indicate the G1/S transition[8]. Time courses of these biomarker proteins under different conditions are given in Figure S4 and S5. Our simulation shows that these cells (pheromone-exposed cells in 0 nM final α-factor) reach the G1/S point in approximately 50 min (Figure S4A). The result for pheromone-exposed cell in 50 nM final α-factor is also supplied (Figure S4B). Moreover, it is observed that when the pheromone is added before 21 min (Figure S5 A and B), the protein Whi5 (nucleus) is produced at high levels, indicating mating arrest. By contrast, when the pheromone is added after 21 min (see Figure S5 D), the protein Cln1/2 is produced at high levels, and the level of Whi5 decreases. These changes imply cell cycle commitment. What's more,

G1/S transition occurs after pheromone-arrested cell reenters cell cycle, which is determined by a sharp switch between high and low levels of Clb5/6 and Sic1. Interestingly, when 240 nM pheromone is added at 21 min (nearly at critical addition time for pheromone-arrested cells), the falling Whi5 increases again (see Figure S5 C), maybe it is more difficult to determinate whether mating arrest or cell cycle.

Apparently, comparing with cycling cell, the results are similar. However, the timing of reentering cell cycle and the duration of G1 phase are both increased.

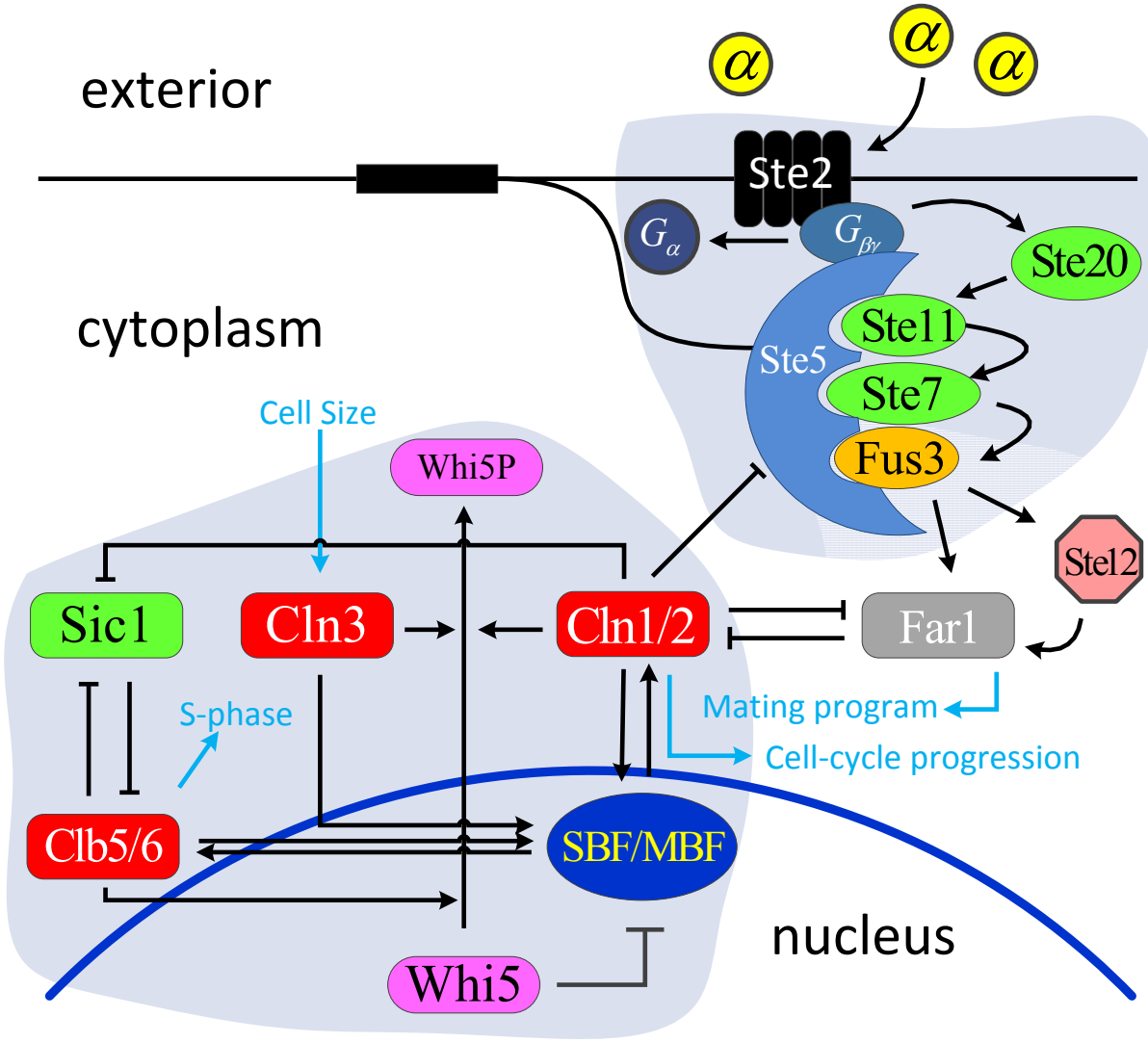

Figure S1 Schematics of the G1 cell cycle pathway and the pheromone-induced MAPK regulatory pathway. The bar-headed lines indicate mutual inhibition (redrawn from Ref.[6-8, 22]).

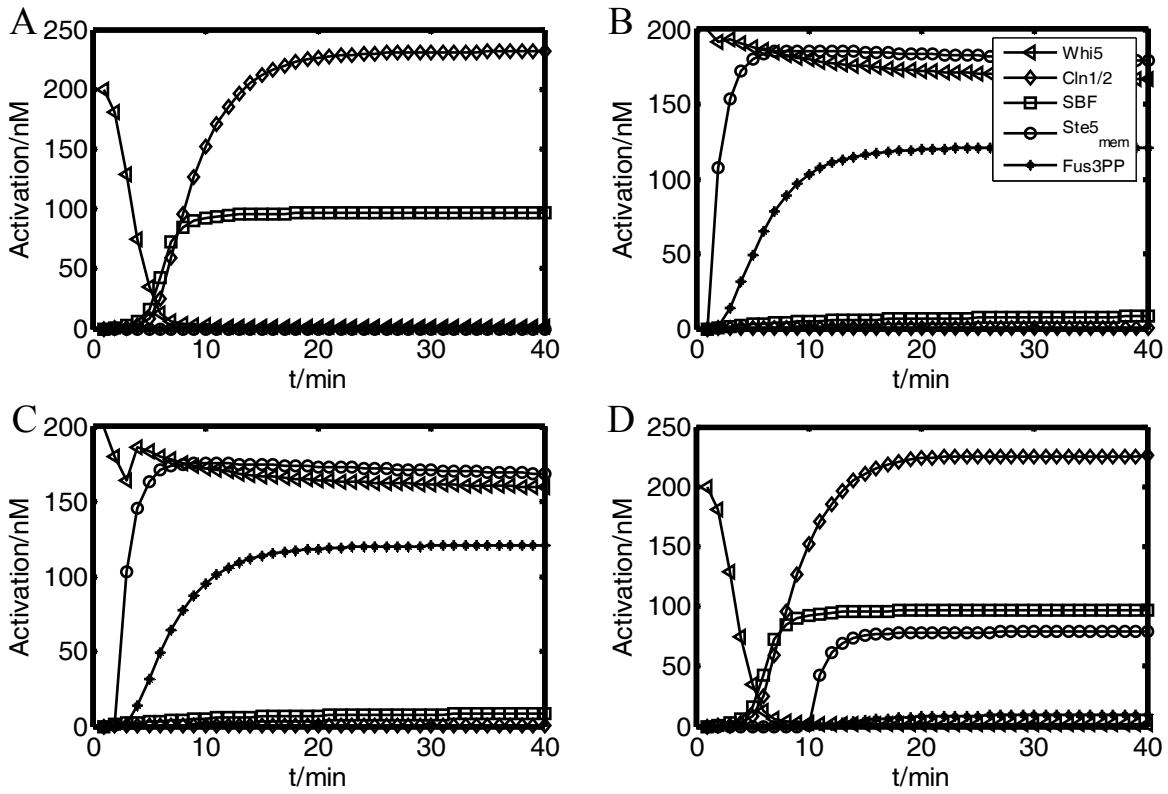

FIGURE S2 Time courses of the wild-type cycling cells. (A) No pheromone is added. (B) Pheromone is added at 0 min. (C) Pheromone is added at 2 min. (D) Pheromone is added at 10 min.

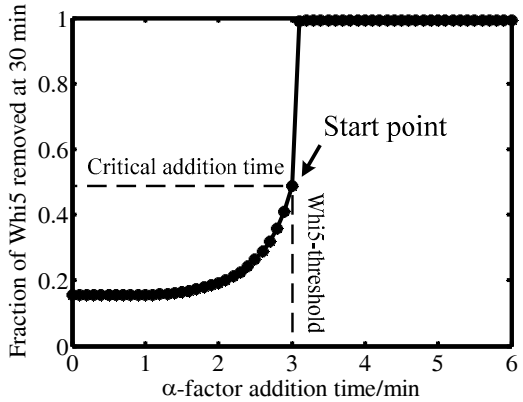

FIGURE S3 Relationship between the time of pheromone addition and Whi5P activation. At the Start point where the maximum slope is achieved in this curve of cell fate decision, there exists one critical addition time that identifies the critical ratio of Whi5 required for a successful transition between two distinct cell fates. In WT cells, Start is defined by the export of approximately half of the nuclear Whi5.

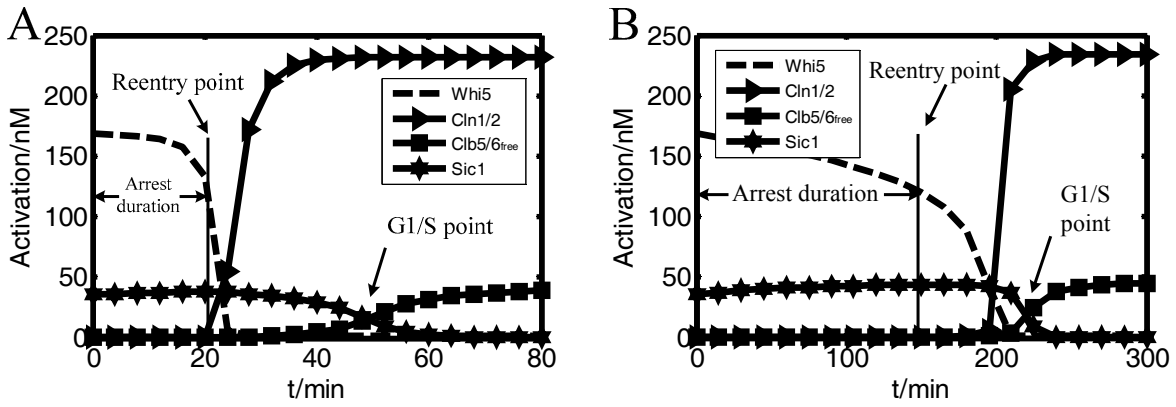

Figure S4. (A).Pheromone-exposed cell in 0 nM final α-factor. (B).Pheromone-exposed cell in 50 nM final α-factor

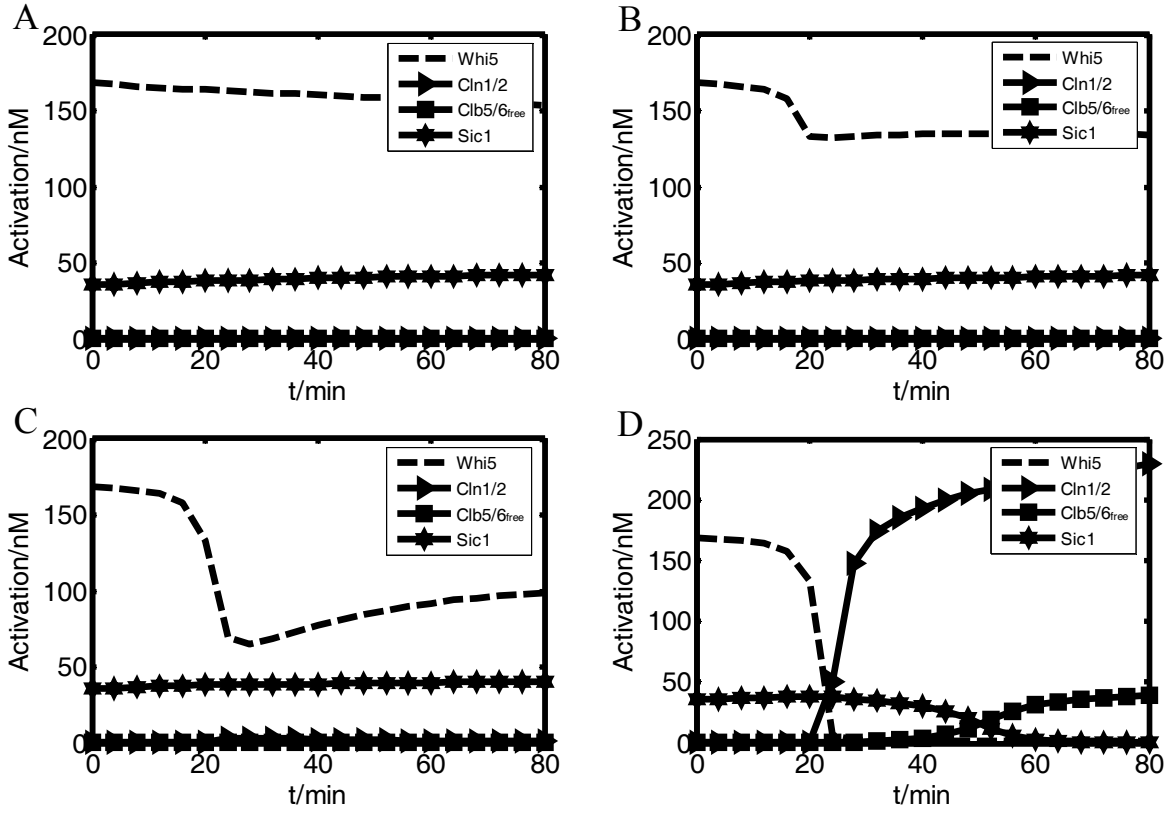

Figure S5. Time courses of pheromone-exposed cells. (A) 240 nM pheromone is added at 10 min. (B) 240 nM pheromone is added at 20 min. (C) 240 nM pheromone is added at 21 min. (D) 240 nM pheromone is added at 22 min.

Table S1 All reaction rates in the mathematical model

Para	Value	Para	Value
k_1	8.6×10^{-1}nMmin^{-1}fL^{-1}	κ_1	$0.005\,\mathrm{min}^{-1}\,\mathrm{nM}^{-1}$
k_2	1×10^{-3}nMmin^{-1}	κ_2	$0.6\,\mathrm{min}^{-1}$
k_3	0.4nMmin^{-1}	κ_3	$0.021\,\mathrm{min}^{-1}\,\mathrm{nM}^{-1}$
k_4	0.35nMmin^{-1}	κ_4	$0.003\,\mathrm{min}^{-1}\,\mathrm{nM}^{-1}$
k_5	0.3nMmin^{-1}	κ_5	$0.065\,\mathrm{min}^{-1}\,\mathrm{nM}^{-1}$
k_6	0.5nMmin^{-1}	κ_6	$4\,\mathrm{min}^{-1}$
k_7	0.1nMmin^{-1}	κ_7	$3\,\mathrm{min}^{-1}$
k_8	4nMmin^{-1}	κ_8	$0.003\,\mathrm{min}^{-1}\,\mathrm{nM}^{-1}$
k_9	0.001nMmin^{-1}	κ_9	$1\,\mathrm{min}^{-1}$
k_{10}	3.5nMmin^{-1}	κ_{10}	$3\,\mathrm{min}^{-1}\,\mathrm{nM}^{-1}$
k_{11}	2nMmin^{-1}	κ_{11}	$3\,\mathrm{min}^{-1}\,\mathrm{nM}^{-1}$
k_{12}	6min^{-1}	κ_{12}	$0.05\,\mathrm{min}^{-1}\,\mathrm{nM}^{-1}$
k_{13}	0.152nM^{-1}	κ_{13}	$1\,\mathrm{min}^{-1}$
k_{14}	1.68nM^{-1}	κ_{14}	$20\,\mathrm{min}^{-1}$
k_{15}	0.83nM^{-1}	κ_{15}	$47\,\mathrm{min}^{-1}$
k_{16}	4nM^{-1}min^{-1}	κ_{16}	$50\,\mathrm{min}^{-1}$
k_{17}	1×10^{-4}nMmin^{-1}	κ_{17}	$50\,\mathrm{min}^{-1}$
k_{18}	1×10^{-2}nMmin^{-1}	κ_{18}	$2.5\,\mathrm{min}^{-1}$
k_{19}	7×10^{-3}nMmin^{-1}	κ_{19}	$0.01\,\mathrm{min}^{-1}\,\mathrm{nM}^{-1}$
k_{20}	0.001nMmin^{-1}	κ_{20}	$2\,\mathrm{min}^{-1}$
k_{21}	21nM^{2}min^{-1}	κ_{21}	$3\,\mathrm{min}^{-1}$
k_{22}	0.8nM^{-1}min^{-1}	κ_{22}	$0.25\,\mathrm{min}^{-1}$
k_{23}	0.01min^{-1}	κ_{23}	$0.2\,\mathrm{min}^{-1}$
k_{24}	0.001nMmin^{-1}	κ_{3r}	$0.1\,\mathrm{min}^{-1}$
k_{25}	2nM^{2}min^{-1}	δ_1	$0\,\mathrm{min}^{-1}$

k_{26}	10min^{-1}	δ_2	$0\,\text{min}^{-1}$
k_{27}	10min^{-1}	δ_{ste0}	$0.8\times[\alpha\text{-factor}]/240\,\text{min}^{-1}$
d_1	0.15min^{-1}	δ_{ste1}	$0.7\times[\alpha\text{-factor}]/240\,\text{min}^{-1}$
d_2	0.1min^{-1}	δ_{ste2}	$0.6\times[\alpha\text{-factor}]/240\,\text{min}^{-1}$
d_3	0.3min^{-1}	δ_{ste3}	$0.5\times[\alpha\text{-factor}]/240\,\text{min}^{-1}$
d_4	$3.5\times10^{-2}\text{min}^{-1}$	δ_{ste4}	$0.4\times[\alpha\text{-factor}]/240\,\text{min}^{-1}$
d_5	$1\text{min}^{-1}\text{nM}^{-1}$	δ_{ste5}	$0.3\times[\alpha\text{-factor}]/240\,\text{min}^{-1}$
d_6	$1.54\times10^{-2}\text{min}^{-1}$	δ_{ste6}	$0.2\times[\alpha\text{-factor}]/240\,\text{min}^{-1}$
d_7	$2\times10^{-1}\text{min}^{-1}$	δ_{ste7}	$0.1\times[\alpha\text{-factor}]/240\,\text{min}^{-1}$
d_8	2.4min^{-1}	δ_{ste8}	$0.05\times[\alpha\text{-factor}]/240\,\text{min}^{-1}$
d_9	0.001min^{-1}	γ_0	$0.05\,\text{min}^{-1}$
d_{10}	0.001min^{-1}	γ_1	$0.1\,\text{min}^{-1}$
K_3	8.37×10^{-5}	γ_2	$0.2\,\text{min}^{-1}$
K_4	4.88×10^{-4}	γ_3	$0.3\,\text{min}^{-1}$
K_{18}	0.333×10^{-4}	γ_4	$0.4\,\text{min}^{-1}$
K_{19}	3.01×10^{-4}	γ_5	$0.5\,\text{min}^{-1}$
K_{21}	30nM	γ_6	$0.6\,\text{min}^{-1}$
K_{22}	2000nM	γ_7	$0.7\,\text{min}^{-1}$
K_{25}	1.05nM	γ_8	$0.8\,\text{min}^{-1}$
b	$0.8\text{nM}^{-1}\text{min}^{-1}$		
r	$5\times10^{-1}\text{min}^{-1}$		
λ_1	$0.1\text{nM}^{-1}\,\text{min}^{-1}$		
λ_2	$1.4\times10^{-3}\,\text{nM}^{-1}\,\text{min}^{-1}$		

Table S2 Initial concentrations of all components in the mathematical model

Components	Concentrations (in the model)	Components	Concentrations (in the model)
V	28 fL	Far1	200 nM
Cln3	0 nM	Far1PP	0 nM
Cln1/2	0 nM	α-factor	0~240 nM
SBFT	100 nM	Ste2	200 nM
SBFA	0 nM	Ste5P0	200 nM
MBFT	100 nM	$G_{\alpha\beta\gamma}$	80 nM
MBFP	0 nM	Ste11	158.33 nM
Whi5T	200 nM	Ste7	34 nM
Whi5P	0 nM	Ste20	220 nM
Clb5/6	0 nM	**A**	150 nM
$Clb5/6_{free}$	0 nM	**B**	100 nM
Sic1	30 nM	**C**	150 nM
Ste12	200 nM	Fus3	900 nM
Ste12PP	0 nM		

The concentrations of other components that are not listed in the Table are 0 nM.

SUPPORTING REFERENCES

1. de Bruin R. A. M., McDonald W. H., Kalashnikova T. I., Yates J., Wittenberg C. (2004) Cln3 activates G1-specific transcription via phosphorylation of the SBF transcription bound repressor Whi5. Cell, 117(7), 887-898.
2. Spellman P. T., Sherlock G., Zhang M. Q., Iyer V. R., Anders K., Eisen M. B., Brown P. O., Botstein D., Futcher B. (1998) Comprehensive identification of cell cycle-regulated genes of the yeast Saccharomyces cerevisiae by microarray hybridization. Molecular biology of the cell, 9(12), 3273-97.
3. Cross F. R., Hoek M., McKinney J. D., Tinkelenberg A. H. (1994) Role of Swi4 in cell cycle regulation of CLN2 expression. Molecular and cellular biology, 14(7), 4779-87.
4. Schwob E., Bohm T., Mendenhall M. D., Nasmyth K. (1994) The B-type cyclin kinase inhibitor p40SIC1 controls the G1 to S transition in S. cerevisiae. Cell, 79(2), 233-44.
5. Yang L., MacLellan W. R., Han Z. G., Weiss J. N., Qu Z. L. (2004) Multisite phosphorylation and network dynamics of cyclin-dependent kinase signaling in the eukaryotic cell cycle. Biophysical Journal, 86(6), 3432-3443.
6. Doncic A., Falleur-Fettig M., Skotheim J. M. (2011) Distinct Interactions Select and Maintain a Specific Cell Fate. Molecular Cell, 43(4), 528-539.
7. Li Y. K., Yi M., Zou X. F. (2013) Identification of the molecular mechanisms for cell-fate selection in budding yeast through mathematical modeling. Biophysical Journal, 104(10), 2282-2294.
8. Yang X. J., Lau K. Y., Sevim V., Tang C. (2013) Design principles of the yeast G1/S switch. Plos Biology, 11(10), e1001673.
9. Nash P., Tang X. J., Orlicky S., Chen Q. H., Gertler F. B., Mendenhall M. D., Sicheri F., Pawson T., Tyers M. (2001) Multisite phosphorylation of a CDK inhibitor sets a threshold for the onset of DNA replication. Nature, 414(6863), 514-521.

10. Feldman R. M., Correll C. C., Kaplan K. B., Deshaies R. J. (1997) A complex of Cdc4p, Skp1p, and Cdc53p/cullin catalyzes ubiquitination of the phosphorylated CDK inhibitor Sic1p. Cell, 91(2), 221-30.
11. Koivomagi M., Valk E., Venta R., Iofik A., Lepiku M., Balog E. R. M., Rubin S. M., Morgan D. O., Loog M. (2011) Cascades of multisite phosphorylation control Sic1 destruction at the onset of S phase. Nature, 480(7375), 128-31.
12. Skowyra D., Craig K. L., Tyers M., Elledge S. J., Harper J. W. (1997) F-box proteins are receptors that recruit phosphorylated substrates to the SCF ubiquitin-ligase complex. Cell, 91(2), 209-19.
13. Chang F., Herskowitz I. (1990) Identification of a gene necessary for cell cycle arrest by a negative growth factor of yeast: FAR1 is an inhibitor of a G1 cyclin, CLN2. Cell, 63(5), 999-1011.
14. Wiget P., Shimada Y., Butty A. C., Bi E. R., Peter M. (2004) Site-specific regulation of the GEF Cdc24p by the scaffold protein Far1p during yeast mating. Embo Journal, 23(5), 1063-1074.
15. Lamson R. E., Winters M. J., Pryciak P. M. (2002) Cdc42 regulation of kinase activity and signaling by the yeast p21-activated kinase Ste20. Molecular and Cellular Biology, 22(9), 2939-2951.
16. Whiteway M. S., Wu C., Leeuw T., Clark K., Fourest-Lieuvin A., Thomas D. Y., Leberer E. (1995) Association of the yeast pheromone response G protein beta gamma subunits with the MAP kinase scaffold Ste5p. Science (New York, NY), 269(5230), 1572-5.
17. Kofahl B., Klipp E. (2004) Modelling the dynamics of the yeast pheromone pathway. Yeast, 21(10), 831-850.
18. Shao D. Y., Zheng W., Qiu W. J., Qi O. Y., Tang C. (2006) Dynamic studies of scaffold-dependent mating pathway in yeast. Biophysical Journal, 91(11), 3986-4001.
19. Garrenton L. S., Braunwarth A., Irniger S., Hurt E., Kunzler M., Thorner J. (2009) Nucleus-Specific and cell cycle-regulated degradation of mitogen-activated protein kinase scaffold protein Ste5 contributes to the control of signaling competence. Molecular and Cellular Biology, 29(2), 582-601.
20. Oehlen L. J., McKinney J. D., Cross F. R. (1996) Ste12 and Mcm1 regulate cell cycle-dependent transcription of FAR1. Molecular and cellular biology, 16(6), 2830-7.
21. Elion E. A., Satterberg B., Kranz J. E. (1993) FUS3 phosphorylates multiple components of the mating signal transduction cascade: evidence for STE12 and FAR1. Molecular biology of the cell, 4(5), 495-510.
22. Doncic A., Skotheim J. M. (2013) Feedforward regulation ensures stability and rapid reversibility of a cellular state. Molecular Cell, 50(6), 856-868.
23. Gartner A., Jovanovic A., Jeoung D. I., Bourlat S., Cross F. R., Ammerer G. (1998) Pheromone-dependent G1 cell cycle arrest requires Far1 phosphorylation, but may not involve inhibition of Cdc28-Cln2 kinase, in vivo. Molecular and cellular biology, 18(7), 3681-91.
24. McKinney J. D., Chang F., Heintz N., Cross F. R. (1993) Negative regulation of FAR1 at the Start of the yeast cell cycle. Genes & development, 7(5), 833-43.
25. Takahashi S., Pryciak P. M. (2008) Membrane localization of scaffold proteins promotes graded signaling in the yeast MAP kinase cascade. Current Biology, 18(16), 1184-1191.
26. Skotheim J. M., Di Talia S., Siggia E. D., Cross F. R. (2008) Positive feedback of G1 cyclins ensures coherent cell cycle entry. Nature, 454(7202), 291-6.